J. Fluid Mech. (1974), *vol.* 66, *part* 4, *pp.* 641–655
Printed in Great Britain

Three-dimensional laminar boundary layers in crosswise pressure gradients

By J. H. HORLOCK,
Engineering Department, University of Cambridge†

A. K. LEWKOWICZ
Department of Mechanical Engineering, University of Liverpool

AND J. WORDSWORTH
INTERATOM, Bensberg, Cologne

(Received 20 July 1973 and in revised form 7 June 1974)

Two attempts were made to develop a three-dimensional laminar boundary layer in the flow over a flat plate in a curved duct, establishing a negligible streamwise pressure gradient and, at the same time, an appreciable crosswise pressure gradient.

A first series of measurements was undertaken keeping the free-stream velocity at about 30 ft/s; the boundary layer was expected to be laminar, but appears to have been transitional. As was to be expected, the cross-flow in the boundary layer decreased gradually as the flow became progressively more turbulent.

In a second experiment, at a lower free-stream velocity of approximately 10 ft/s, the boundary layer was laminar. Its streamwise profile resembled closely the Blasius form, but the cross-flow near the edge of the boundary layer appears to have exceeded that predicted theoretically. However, there was a substantial experimental scatter in the measurements of the yaw angle, which in laminar boundary layers is difficult to obtain accurately.

1. Introduction

An understanding of the development of the three-dimensional boundary layers on compressor and turbine blades is required if blade sections are to be designed for minimum loss. At the Reynolds numbers attained in practice, a laminar boundary layer may be preserved for a short distance on a compressor blade, before laminar separation or transition takes place. On turbine blades extended areas of laminar flow are possible (see Horlock 1969). A general solution of the equations describing the laminar boundary layer on a blade rotating in a radial pressure gradient has been given (Horlock & Wordsworth 1965) and the initial object of the experiments described here was to provide measurements for comparison with this solution.

Figure 1 shows the helical co-ordinate system that was used for the original

† Present address: University of Salford, Salford M5 4WT, England.

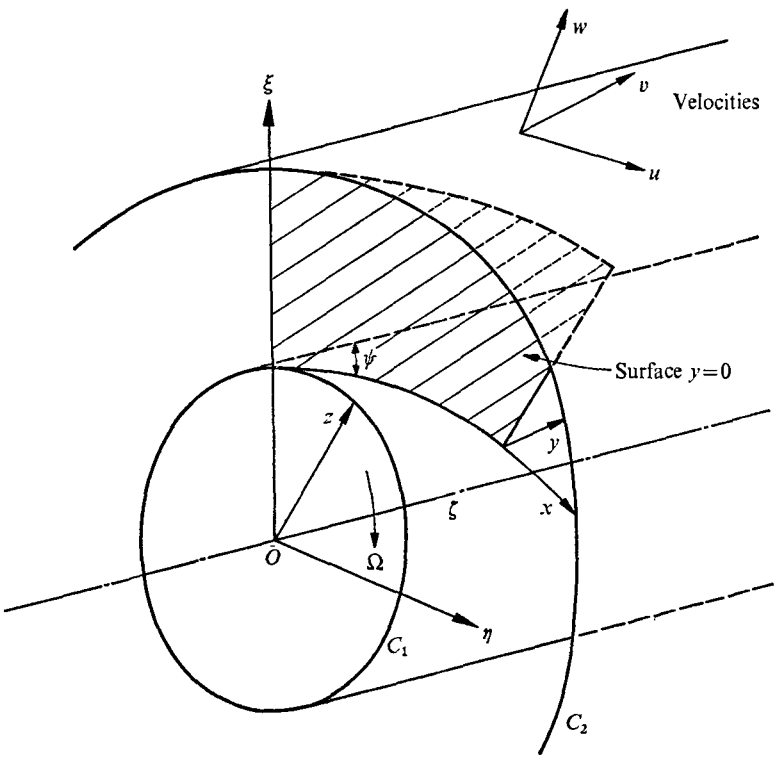

FIGURE 1. The helical blade.

theoretical investigation. The helical blade lies in the surface $y = 0$. As in an axial turbomachine, the fluid flows in an annular region between an inner cylinder C_1, rotating about the ζ axis, and an outer fixed cylinder C_2; the helical blade projects from the surface of C_1. The construction of an experimental rig to test the helical-blade analysis is a formidable task. It would be extremely difficult to manufacture the blade, and a reliable pressure-transmission device would have to be developed if measurements of the boundary layer on the rotating blade were to be made. It was therefore decided to use a non-rotating system, and to take the simplest case of $\psi = 90°$: a stationary flat plate in a near free vortex flow.

It was experimentally convenient to build the test rig so that the ζ axis (as defined in figure 1) was vertical. Then, with $\Omega = 0$ and $\psi = 90°$, the cylinders C_1 and C_2 become vertical circular walls curved about a common axis of curvature (the ζ axis), and the helical blade ($y = 0$) becomes a flat plate in a horizontal plane (see figure 2, which shows the geometry adopted).

Experiments with three-dimensional laminar boundary layers are very difficult as low flow velocities must be maintained, so that measuring instruments, such as total pressure yawmeters, have reduced sensitivity. In order to obtain the largest possible measurements of velocity, a first series of experiments was conducted with a free-stream velocity of approximately 30 ft/s, at which substantial areas of laminar flow were expected. However, it was found that at

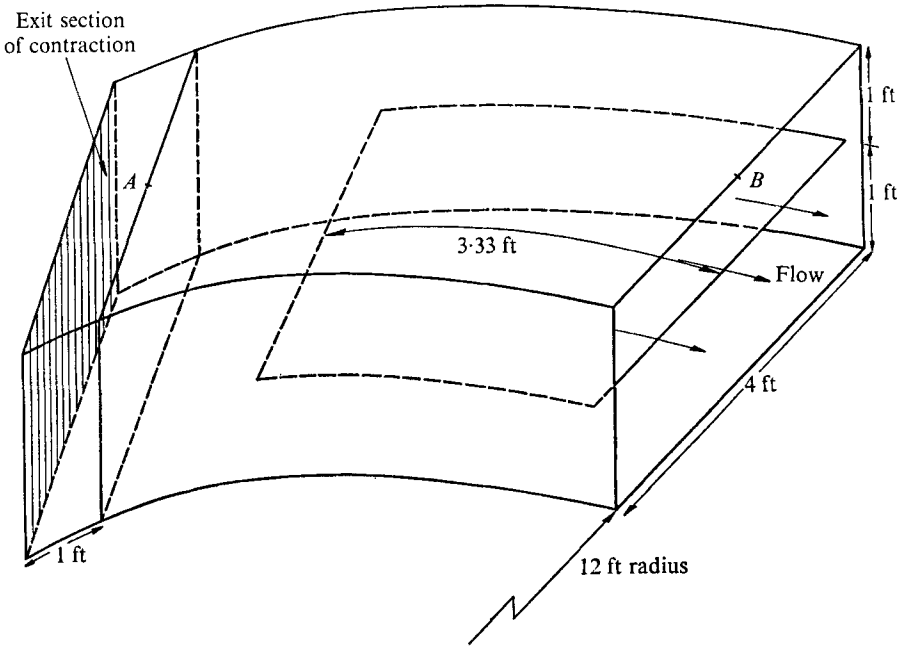

FIGURE 2. First experiment: the curved duct and flat plate. Arc length $AB = 5$ ft.

this velocity the boundary-layer flow was transitional so it was subsequently decided to stage another set of measurements for which the free-stream velocity was lowered to about 10 ft/s. A considerable time elapsed between the two experiments, and when the second experiment was decided upon the original equipment was no longer available. For this reason the second experiment was carried out in a different wind tunnel with a new curved duct and flat plate. These had the same basic dimensions as the original duct and plate but differed in construction, material and minor detail.

The two experiments are discussed separately and the respective results are individually compared with the Horlock–Wordsworth analysis.

2. First experiment

Experimental apparatus and instrumentation

A blower wind tunnel, as designed and described by Gibson (1960), was used in the first experiment. The air velocity at the exit from the contraction could be held steady at any value up to 100 ft/s and the intensity of turbulence at this section was about 0·25 % (see Shaw, Lewkowicz & Gostelow 1966).

The boundary layer was developed on a flat plate placed in a curved duct of constant cross-section (4 + 2 ft) attached to the exit from the wind-tunnel contraction (see figure 2). The vertical side walls of the duct were of constant radii, 12 ft and 16 ft respectively.

The plate, made of 0·25 in. thick hardboard, 4 ft across and of 3·33 ft chord

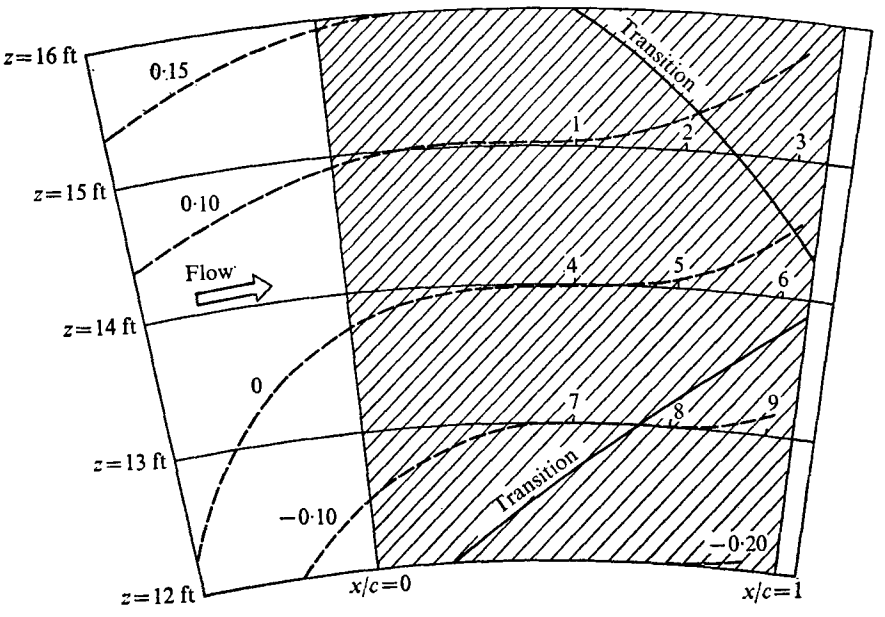

FIGURE 3. First experiment: contours of static pressure $(p-p_a)/(p_0-p_a)$ in the duct, transition lines on the flat plate and measuring stations 1–9.

at the mean radius, was supported by six aerofoil-sectioned struts resting on the bottom wall. The top of the leading edge was smoothed off (to give a semi-aerofoil shape) in order to secure the position of the stagnation point on the upper surface of the plate and to avoid undesirable leading-edge separation.

Static pressure tappings were provided on the curved side walls of the duct at intervals of approximately 3 in., in a row parallel to the plate and half-way between the plate and top wall (i.e. 6 in. above the plate). Further sets of static pressure tappings were provided on the plate at radii of 13, 14 and 15 ft.

A special instrument was designed for boundary-layer measurements; it comprised a traversing and yawing mechanism which carried a replaceable hypodermic probe (Pitot tube or claw yawmeter). The probe could be inserted vertically through the top wall of the duct on arcs of radii 13, 14 and 15 ft at intervals of approximately 3 in. The positions of the static pressure tappings on the plate coincided with the position of the head of the probe inserted through the top wall.

In this experiment the yawmeter was first used at each of the nine test stations, as shown in figure 3 (numbers 1–9), to trace the direction of flow inside and outside the boundary layer. Pitot-tube traverses were made subsequently.

Qualitative observations

Initially smoke was used to visualize the flow at a nominal free-stream velocity of 10 ft/s. At this flow velocity, a laminar boundary layer extended over most of the flat plate. A smoke generator (of the type developed by Preston & Sweeting

1943) was used; this apparatus allows the intensity of the trace filament to be controlled as required. Trace filaments were introduced into the air stream via two static tappings in the flat plate; these lay close together near the leading edge on the central arc of radins 14 ft. The tappings were connected in parallel to the smoke generator, and the rates of flow of smoke in the leads adjusted until one filament was contained by the boundary layer and the other filament just reached the free stream. Boundary-layer and free-stream flows could thus be observed simultaneously. The streamlines were photographed without difficulty in a streamwise direction by directing the illumination along the filaments (figure 4, plate 1).

The analysis of Horlock & Wordsworth shows that at any given chordwise location x the deviation of any streamline in the boundary layer (from the free-stream flow direction) should be independent of the Reynolds number. A calculation using this analysis gave a deviation ϵ_0 at the wall of $22\frac{1}{2}°$ near the trailing edge of the plate. The smoke line in the boundary layer showed a smaller deviation ($\epsilon = 18°$), but since the smoke line must be at a finite distance from the wall, this difference is not unexpected. The china-clay technique developed by Richards & Burstall (1945) was then used to check whether laminar flow could be achieved at a higher velocity ($U \simeq 30$ ft/s) at which quantitative measurements could be made more easily. Schlichting (1955, p. 310) suggests a transition Reynolds number of about $3–5 \times 10^5$ depending on turbulence intensity, so laminar flow was expected over about the first 2 ft of the plate at 30 ft/s. The tunnel was run at this speed and, after a short time, the china-clay pattern showed good contrast between laminar and turbulent regions (figure 5, plate 1). To test the technique the laminar boundary layer was also tripped with a wire. Clear white patches were obtained immediately downstream of the wire, confirming that the china-clay technique gave a ready means of identifying a turbulent area.

The approximate position of the transition line observed on the plate photographically is retraced to scale in figure 3. On the basis of this evidence it was expected that at stations 1, 4, 7 and 5 reasonable laminar boundary-layer profiles would be developed at a free-stream velocity of 30 ft/s. This supposition proved to be false, as will be seen later, probably because the china-clay transition patterns obtained (figure 5) represented the end of transition rather than the transition front. The front must have been located some way upstream of the measuring stations, forming a wide transition zone. This is indicated by the quantitative results described below.

Quantitative measurements (at 30 ft/s)

Boundary-layer profiles were measured at all nine stations indicated in figure 3. The local streamwise boundary-layer velocities were calculated from the values of the local dynamic pressure, being the difference between the Pitot total pressure and the corresponding wall static pressure. Since the values of the boundary-layer yaw angle never exceeded 15° and since Pitot tubes are known to register total pressures within 1 % for yaw angles up to about $\pm 20°$ (see Liepmann & Roshko 1957, p. 148), the Pitot tube was not rotated from the free-stream direction.

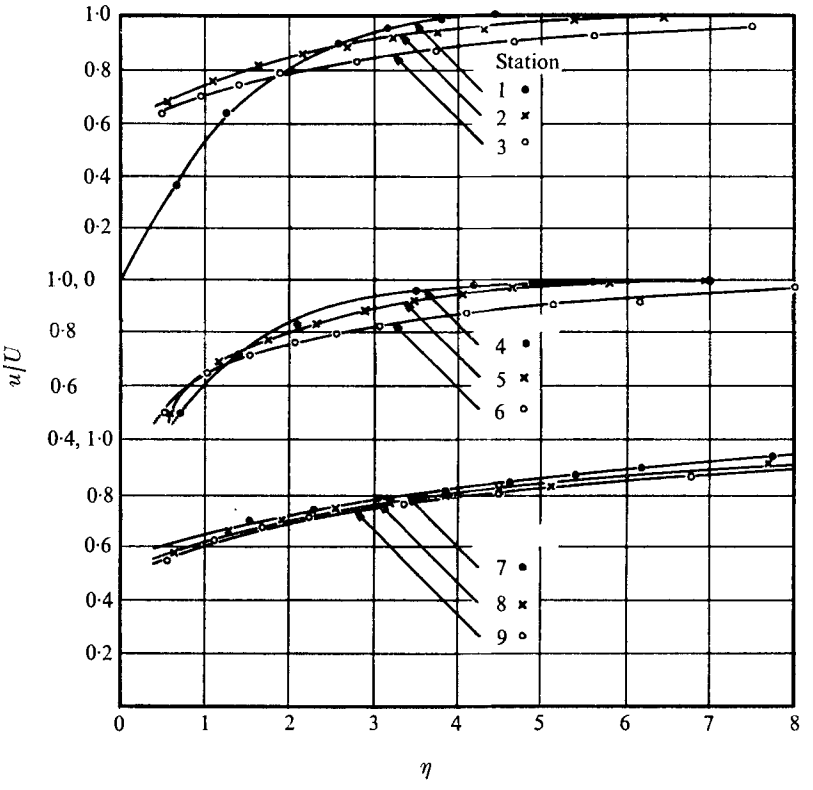

FIGURE 6. Streamwise velocity profiles at stations 1–9.

The Young & Maas (1936) correction for the displacement of the effective centre of the tube was in this case generally negligible (0·006 in.) and was ignored.

The free-stream pressure distribution on the plate is shown in figure 3 in the form of contours of $(p-p_a)/(p_0-p_a)$, where p_a is atmospheric pressure and p_0 is the stagnation pressure at the entry to the test section. There is a slight departure from the 'radial equilibrium' condition (i.e. from circumferential streamlines) in parts of the curved duct; considering the relatively small turning angle of the duct this is not surprising. Figure 6 shows the streamwise velocity profiles (u/U against η) for all nine stations, where U is the free-stream velocity and η is the Blasius transverse co-ordinate ($\eta = y(U/\nu x)^{\frac{1}{2}}$, in which y = distance from wall, x = distance from leading edge along streamline and ν = kinematic viscosity). Figure 7 presents the corresponding yaw-angle profiles, ϵ against η.

Discussion

A calculation of the laminar velocity profiles was made using the analysis of Horlock & Wordsworth (1965). It is assumed in this analysis that there is no streamwise pressure gradient and this assumption is therefore implied in the calculation, so that for small cross-flows the Blasius solution results for the

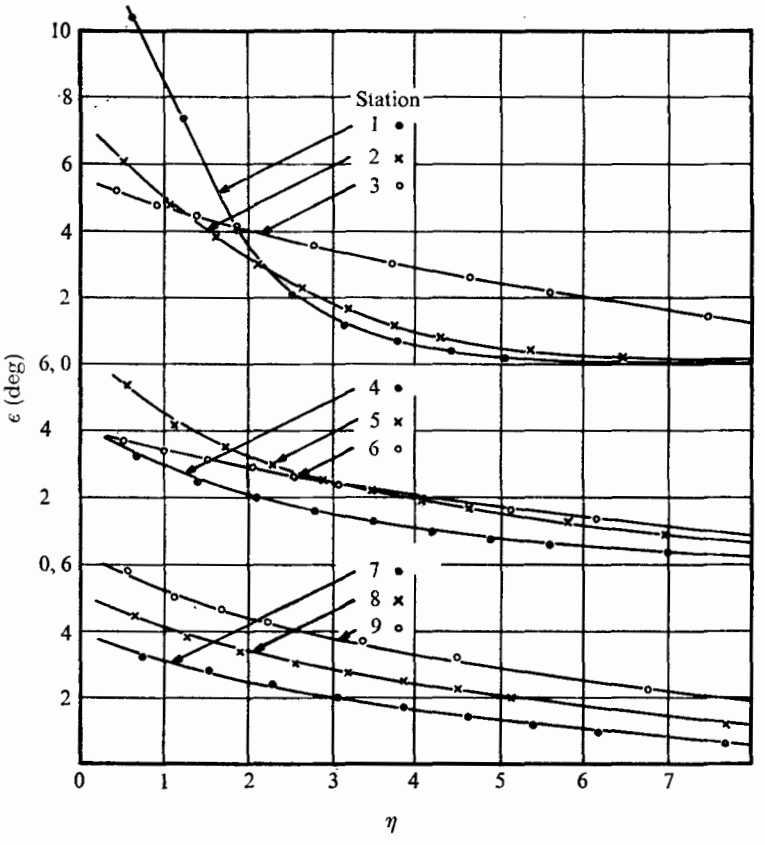

FIGURE 7. Yaw-angle profiles at stations 1–9.

velocity profile in the direction of the mainstream flow. For calculation of the cross-flow the curvature of the streamlines is required and, rather than using the geometrical curvature $1/R$ of circular arcs on the plate, approximate values of the streamline curvature

$$K = \frac{1}{U}\left(\frac{\partial U}{\partial z}\right)_x = \frac{1}{\rho U^2}\left(\frac{\partial p}{\partial z}\right)_x$$

were obtained from the static pressure contours. Here z is the crosswise co-ordinate, so that $(\partial p/\partial z)_x$ is the radial pressure gradient at a point a distance x from the leading edge. The distance x is measured along the circular arcs, the difference between the distance from the leading edge measured along the streamlines and along the circular arcs being negligible. The streamlines did not attain a free vortex condition in the duct and $1/K$ was greater than R.

Figure 8 shows the calculated flow at station 1 ($x/c = 0{\cdot}494$, $z/c = 4{\cdot}57$, where c is the chord on the central arc) compared with that observed. The yaw angle ϵ through the boundary layer is quite well predicted, but the observed streamwise velocity profile u/U is 'fuller' than the Blasius profile. With the exception of station 4, the discrepancies between the laminar boundary-layer theory and experiment at the stations are substantial.

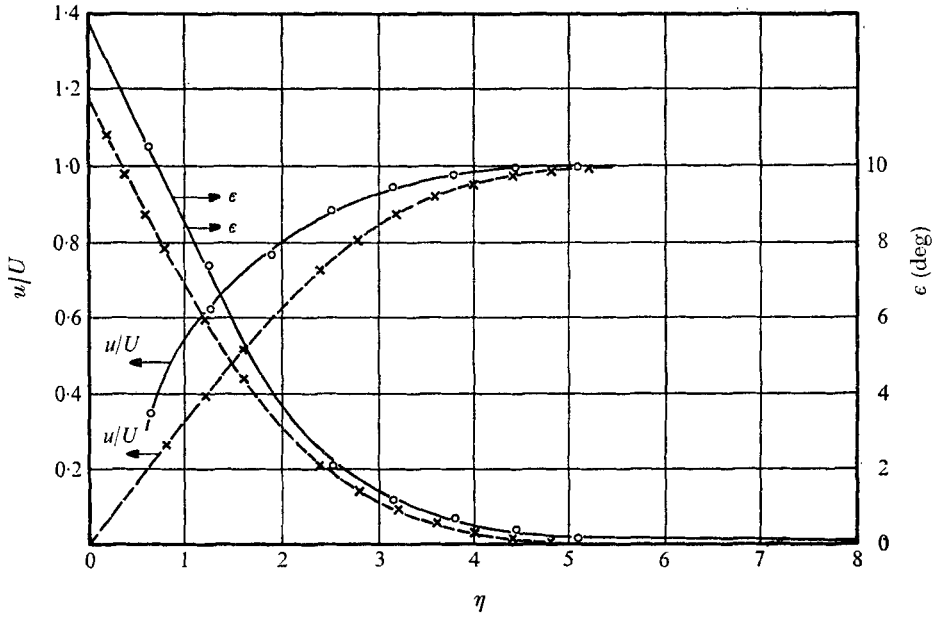

FIGURE 8. Streamwise velocity and yaw-angle profiles at station 1.
———, experimental values; – – –, theoretical solution.

Assuming the flow to be laminar, two possible reasons for the discrepancy between theory and experiment were considered.

(i) The stagnation point might be located some way downstream from the leading edge of the plate. However, in order to match the velocity profiles observed at stations 4 and 5 with the Blasius profile, it was necessary to assume that the laminar boundary layer started from a point about 1 ft from the leading edge, which was not acceptable.

(ii) The boundary layer was subjected to a slightly accelerating flow over about the first 2 ft of the plate (see figure 5) so the assumption of a Blasius profile developing in the streamwise direction might be invalid. Cooke & Hall (1962) have given an approximate Polhausen method for calculating three-dimensional laminar boundary layers under such conditions. Their analysis was applied using the observed pressure gradient (assuming a linear velocity variation between $x = 0$ and $x = 2$ ft). A Polhausen parameter $(\delta^2/\nu)\,dU/dx$ of 0·05 was obtained, and it was found that the thickness of the boundary layer at station 4 would be only some 2 % less than if it grew under zero pressure gradient. Furthermore, the effect on the velocity profile was negligible. It appeared therefore that the experimental conditions did, to all practical purposes, meet the requirement of zero pressure gradient.

Thus, although the evidence from the china-clay tests suggested that the flow was laminar over much of the plate, the quantitative measurements (figure 6) indicated that the flow was in transition at stations 2, 3 and 6–9 and probably at stations 4 and 5. Indeed, transition had probably just begun even at station 1. The method of Dhawan & Narasimha (1958) for deriving velocity profiles in

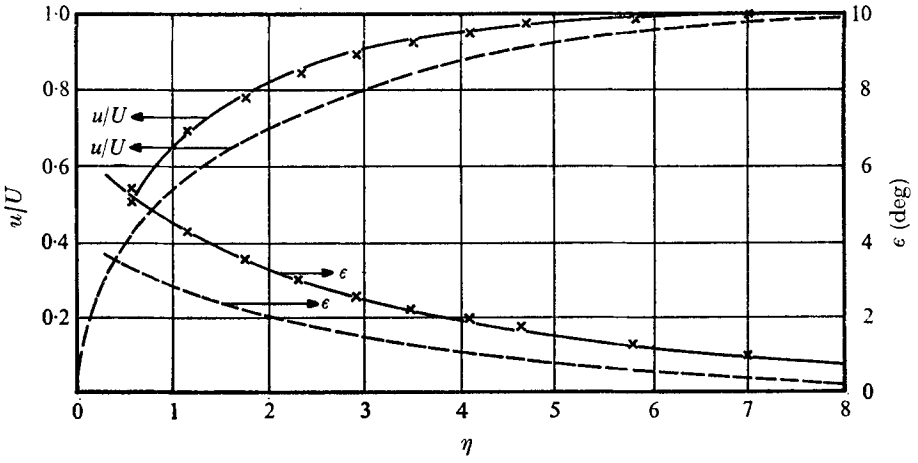

FIGURE 9. Streamwise velocity and yaw-angle profiles at station 5. ———, experimental values; – – –, theoretical solution.

such transitional flows was therefore used. If a laminar boundary layer growing from $x = 0$ would produce a velocity profile $u_L(y)$ and a turbulent boundary layer growing from the transition point $x = x_t$ would produce a velocity profile $u_T(y)$, then Dhawan & Narasimha argue that a Pitot tube would record a resultant velocity

$$u_R = (\gamma u_T^2 + (1-\gamma)\, u_L^2)^{\frac{1}{2}},$$

where γ is the intermittency (the fraction of time for which the flow is turbulent), which is a function of the distance along the transition length and may be obtained from a correlation of their data.

Calculations were carried out assuming that transition took place at

$$x_t = 1{\cdot}33 \text{ ft}$$

(i.e. much earlier than the position indicated by the china clay). The three-dimensional laminar flow was calculated from the Horlock & Wordsworth analysis and the turbulent flow was calculated using a method developed by Hoadley (1971). The turbulent streamwise velocity profile may be represented by the Coles approximation, with parameters δ (absolute boundary-layer thickness), π (wake parameter) and c_f (wall friction coefficient), and the yaw-angle profile in turbulent flow by the Prandtl–Mayer approximation $\epsilon_T = \epsilon_0(1-y/\delta)^2$, where ϵ_0 is the deviation between the limiting streamlines. The streamwise and cross-flow momentum integral equations, the entrainment equation and the Coles skin-friction relation were solved simultaneously for δ, π, c_f and ϵ_0, as functions of x.

The streamwise velocity profile u_R/U calculated in this way (for $x_t = 1{\cdot}33$ ft and for $\gamma = 0{\cdot}15$ from the Dhawan & Narasimha correlation) is shown in figure 9, for station 5. The measured profiles are still 'fuller' than the calculated profiles. If it is supposed that the resultant deviation is

$$\epsilon_R = \gamma\epsilon_T + (1-\gamma)\,\epsilon_L,$$

then a resultant value of the deviation may be calculated. In figure 9 such values of ϵ_R are also compared with measurements made at station 5 (for $x_t = 1{\cdot}33$ ft);

the magnitude of the deviation is underestimated although the form of the variation through the boundary layer is predicted correctly. Similar calculations with $x_t = 1{\cdot}00$ ft showed little improvement, although the calculated profile more closely approached a turbulent profile.

The results of this series of tests and calculations suggested that what had been expected to be a laminar three-dimensional boundary layer was probably a transitional boundary layer.

Gregory (1960) has shown that transition in the boundary layer developing over a swept wing may not be a simple 'primary' transition, similar to that observed in two-dimensional flow. He found that transition at the root of the swept wing could occur owing to instability of the secondary flow, and that this 'secondary' transition could move well forward of the primary transition observed further out on the wing. The Reynolds number at primary transition in Gregory's experiment was substantially higher than in the present experiment, but the Reynolds number at his 'secondary' transition points was significantly less. However, the striations due to longitudinal vortices associated with secondary transition by Gregory and by Anscombe & Illingworth (1952) were not observed in the china clay on the flat plate.

3. Second experiment

Experimental apparatus and instrumentation

In view of the difficulties encountered with the original experiment it was decided to repeat the experiment by measuring the boundary layer near the middle of the plate at a lower free-stream velocity of about 10 ft/s. As pointed out in the introduction, the original apparatus was no longer available when these additional measurements were decided upon. A new duct and plate, substantially similar to the original ones, were constructed and connected to another but similar wind tunnel, described by Lewkowicz (1965), with a slightly different turbulence level (of the order of 0·15 %) at the exit from the contraction section. The new duct and plate were fabricated mainly from clear perspex to facilitate visual access into the duct. The new plate was circumferentially a little longer and contained 117 static pressure holes so that the free-stream pressure distribution could be determined more accurately. The plate and the corresponding non-dimensional pressure contours $(p-p_a)/(p_0-p_a)$ are shown in figure 10. As in the original duct the side-wall static pressures could be measured.

More sophisticated arrangements were made for boundary-layer measurements in this second experiment. A special 'cobra' (Pitot-cum-yaw) instrument with a hypodermic head (0·032 in. O.D.) was constructed. It could be fastened locally to the upper plate surface by means of a strong magnet and operated remotely by a set of Bowden cables for both the yaw and traverse adjustments, the respective positions being monitored by two accurate dial gauge micrometers. Both Pitot and yawmeter tubes were connected to two accurate thermally insulated micromanometers with optical magnification of the meniscus and the reference hair-line.

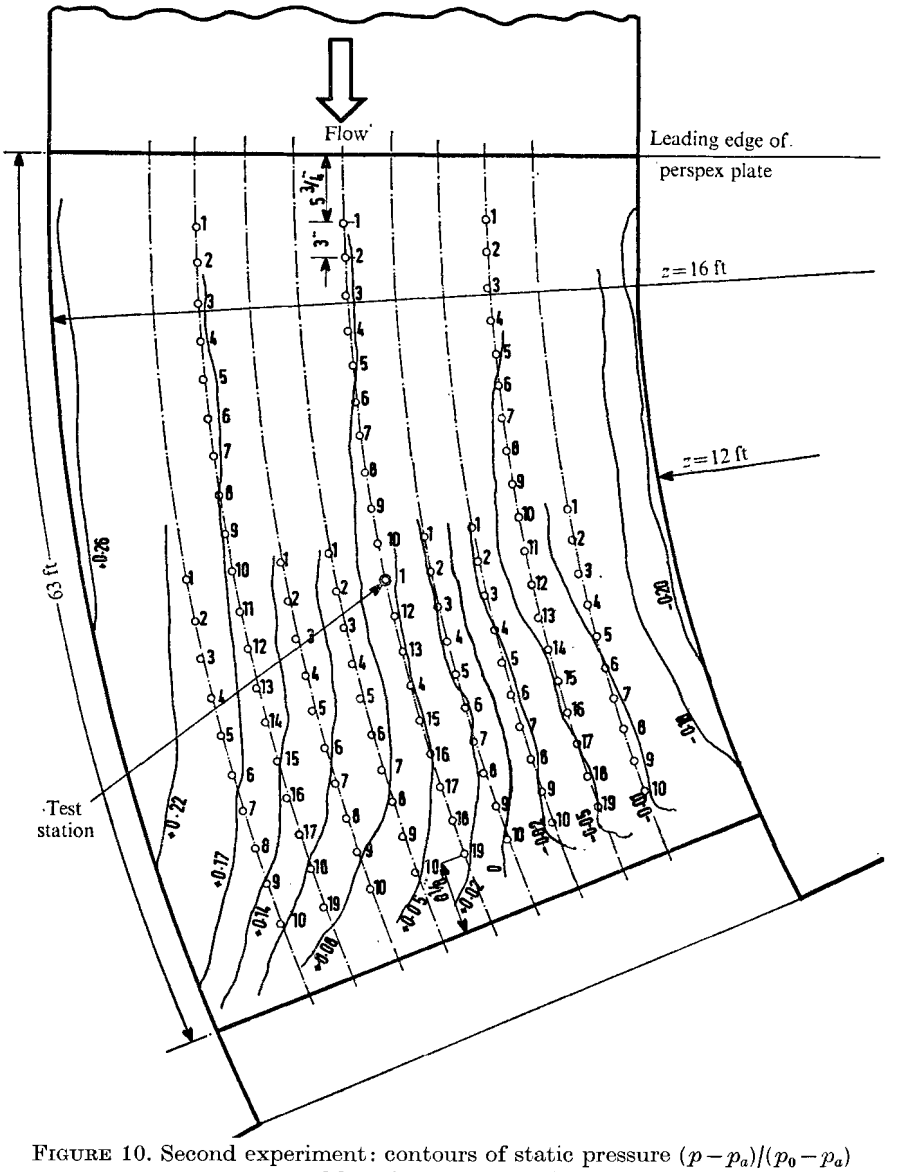

FIGURE 10. Second experiment: contours of static pressure $(p-p_a)/(p_0-p_a)$ and location of test station.

Qualitative and quantitative measurements

The boundary-layer traverses were again preceded by flow visualization using china clay. The flow pattern observed is illustrated in figure 11 (plate 2), which shows a substantially laminar flow over the entire plate. The white patches near the leading edge are due to high rates of evaporation that occur in the areas of high wall friction coefficient. A slightly tapered leading edge on the plate resulted in a localized favourable pressure gradient.

The boundary layer was traversed three times with the Pitot–yawmeter instrument at a test station located at a distance $x = 35{\cdot}75$ in. along the central

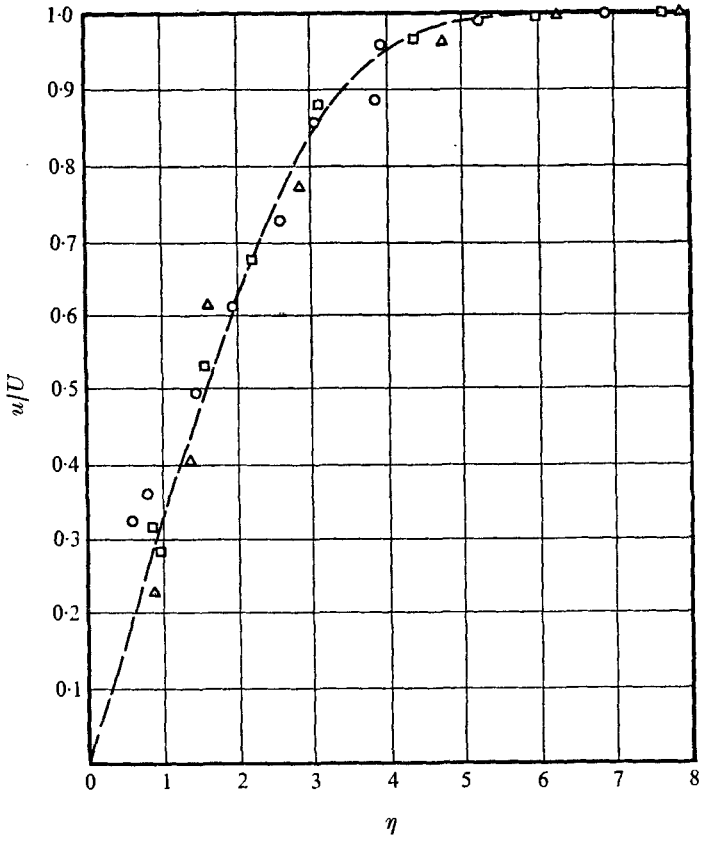

FIGURE 12. Streamwise velocity profile. ○, test 1; △, test 2 (repeat); □, test 3 (repeat); – – –, Blasius profile.

arc (the point is marked in figure 10). The resulting streamwise velocity profile (u/U against η) and the yaw-angle distribution (ϵ against η) are presented in figures 12 and 13, respectively. Both quantities measured are subject to noticeable experimental scatter. In figure 13 points marked '?' seem to deviate conspicuously from the general trend of the ϵ, η curve.

The yaw-angle measurements were very difficult in this experiment. At low air velocities a pressure differential manometer, such as that used here, tends to display a 'hysteresis' type of behaviour when near balance (i.e. near the point of alignment). At worst, an angular insensitivity of $\pm 1°$ was experienced owing to this effect as indicated by the queried points in figure 13. The manometer insensitivity for both Pitot and yaw measurements was less than $\pm 10^{-3}$ in. of water, which seems consistent with the worst scatter in figure 12.

Discussion

While the measured streamwise velocity profile is similar to the expected Blasius distribution (figure 12), the expermiental yaw-angle profile does not agree well with the Horlock–Wordsworth theory. The disparity in ϵ is most noticeable in

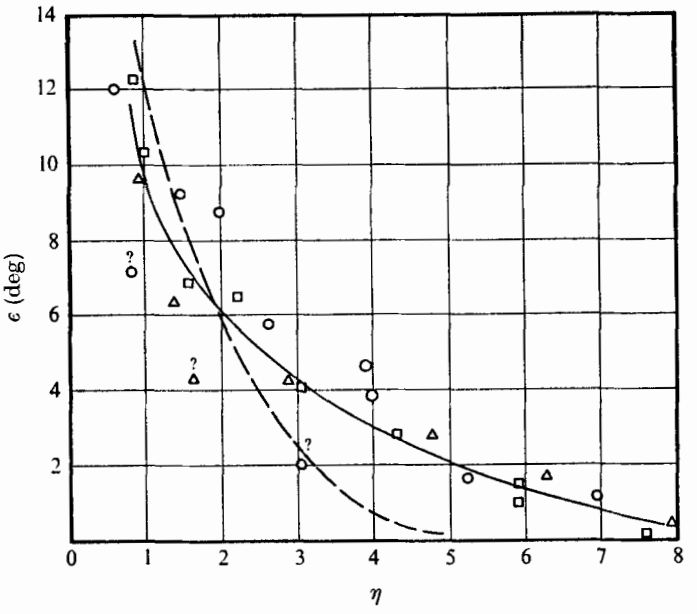

FIGURE 13. Yaw-angle profile. ○, test 1; △, test 2 (repeat); □, test 3 (repeat); – – –, Horlock & Wordsworth ($K = U^{-1}\partial U/\partial z$).

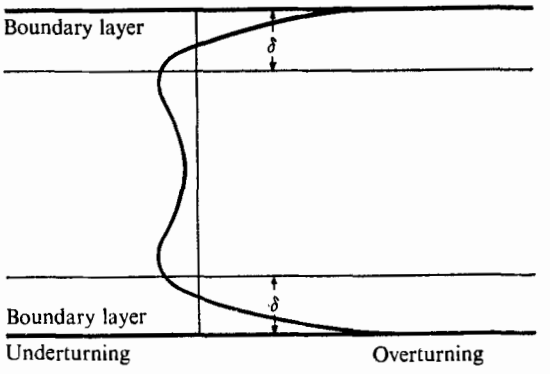

FIGURE 14. Expected flow deviations in bounded ducts.

the range $\eta > 3$, where experimental values consistently exceeded the predicted values by some 2–3°. Moreover, ϵ becomes zero not at $\eta \approx 5$, as expected, but at $\eta \approx 8$, indicating the possibility of some form of 'inviscid' cross-flow outside the boundary layer (compare figures 12 and 13).

There are two possible explanations for such inviscid cross-flows: classical secondary flow developed within the duct above the plate and residual concencentrated swirl originating from the axial flow fan driving the wind tunnel.

Secondary (streamwise) circulations produced by deflexion of the plate boundary layer and by deflexion of the boundary layer on the top wall of the duct will be in opposite directions. The three-dimensional boundary layers are 'bounded' by the curved walls of the duct and there must be a return flow

from the counter-rotating secondary motions, causing an underturning in the mainstream (see Horlock 1973). Classical secondary flows of this type produce a yaw-angle profile as indicated in figure 14, but there is no evidence of this kind of effect, with underturning just outside the boundary layers, in the present experiments. The 'bounding' effect is virtually non-existent because the aspect ratio of the duct (height/width) is very small.

It seems more probable that the overturning outside the boundary layer is due to the residual swirl. There is some evidence for this in previous experiments carried out in the wind tunnel by Lewkowicz (1965). He noticed small angular non-uniformities of flow in the cross-section at the exit from the contraction, which may have persisted in the flow over the plate, especially if they were due to a concentrated 'line' vortex (in this case, the hub vortex of the wind-tunnel fan).

4. Conclusions

Velocity and yaw-angle profiles observed in the laminar boundary layer on a flat plate in a curved duct compared reasonably well with the Horlock–Wordsworth analysis when the free-stream velocity did not exceed 10 ft/s. Some experimental scatter could not be eliminated in spite of carefully designed instrumentation. Some residual swirl in the wind-tunnel contraction appears to mar the comparisons of the experimentally observed yaw-angle profiles with the theoretical predictions.

At a higher free-stream velocity (30 ft/s) flow visualization tests with china clay indicated only small areas of turbulent flow but detailed measurements of the boundary layer, although repeatable, did not show simple laminar flow. It appears that the boundary layer observed at the higher Reynolds number was a three-dimensional variation of the transitional flow observed by Dhawan & Narasimha in a two-dimensional flow.

The authors are indebted to Mr B. C. Ler, who helped to obtain the data shown in figures 10 and 11.

REFERENCES

ANSCOMBE, A. & ILLINGWORTH, L. N. 1952 *Aero. Res. Counc. R. & M.* no. 2968.

COOKE, J. & HALL, M. 1962 Boundary layers in three dimensions. *Prog. Aero. Sci.* **2**, 221–282.

DHAWAN, S. & NARASIMHA, R. 1958 *J. Fluid Mech.* **3**, 418–436.

GIBSON, M. M. 1960 Ph.D. thesis, Liverpool University.

GREGORY, N. 1960 *J. Roy. Aero. Soc.* **63**, 562–564.

HOADLEY, D. 1971 Boundary layer development in an annular diffuser. I. *Mech. E. Proc. Symp. on Internal Flow, Salford University*, paper 4, A19.

HORLOCK, J. H. 1969 In *Flow Research on Blading* (ed. L. S. Dzung), pp. 322–371. Elsevier.

HORLOCK, J. H. 1973 *J. Mech. Engng Sci.* **15**, 274–284.

HORLOCK, J. H. & WORDSWORTH, J. 1965 *J. Fluid Mech.* **23**, 305–314.

LEWKOWICZ, A. K. 1965 Ph.D. thesis, Liverpool University.

LIEPMANN, H. W. & ROSHKO, A. 1957 *Elements of Gasdynamics*. Wiley.

PRESTON, J. H. & SWEETING, N. E. 1943 *Aero Res. Counc. R. & M.* no. 2023.

RICHARDS, E. J. & BURSTALL, F. H. 1945 *Aero. Res. Counc. R. & M.* no. 2136.

SCHLICHTING, H. 1955 *Boundary Layer Theory*, 4th edn. McGraw-Hill.

SHAW, R., LEWKOWICZ, A. K. & GOSTELOW, J. P. 1966 *Aero. Res. Counc. Current Paper*, no. 847.

YOUNG, A. D. & MAAS, J. N. 1936 *Aero. Res. Counc. R. & M.* no. 1770.

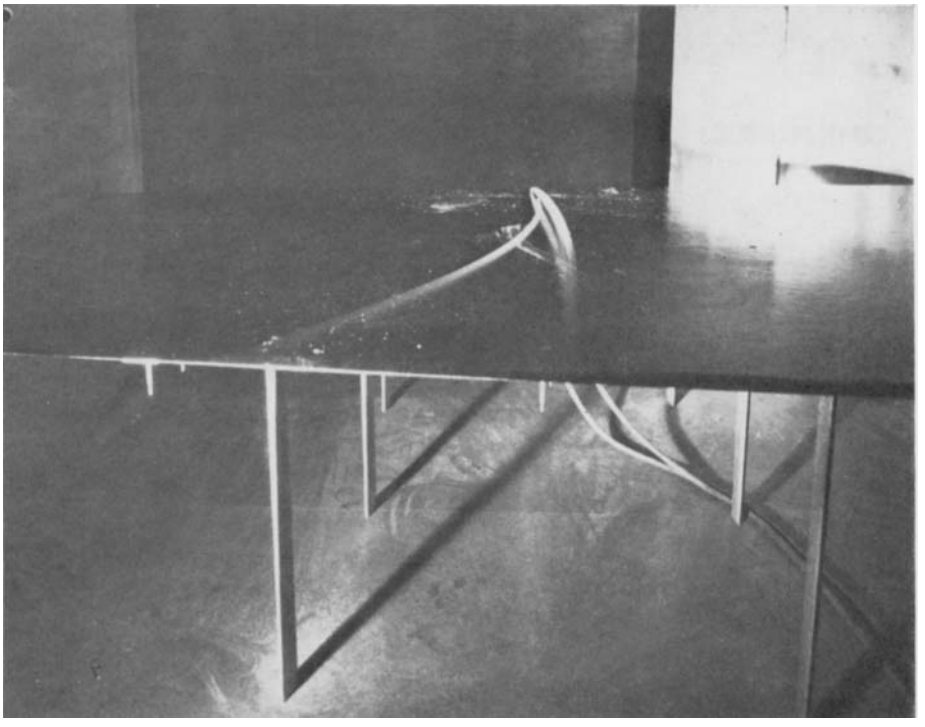

FIGURE 4. Smoke filaments at $U \simeq 10$ ft/s. (View in an upstream direction.)

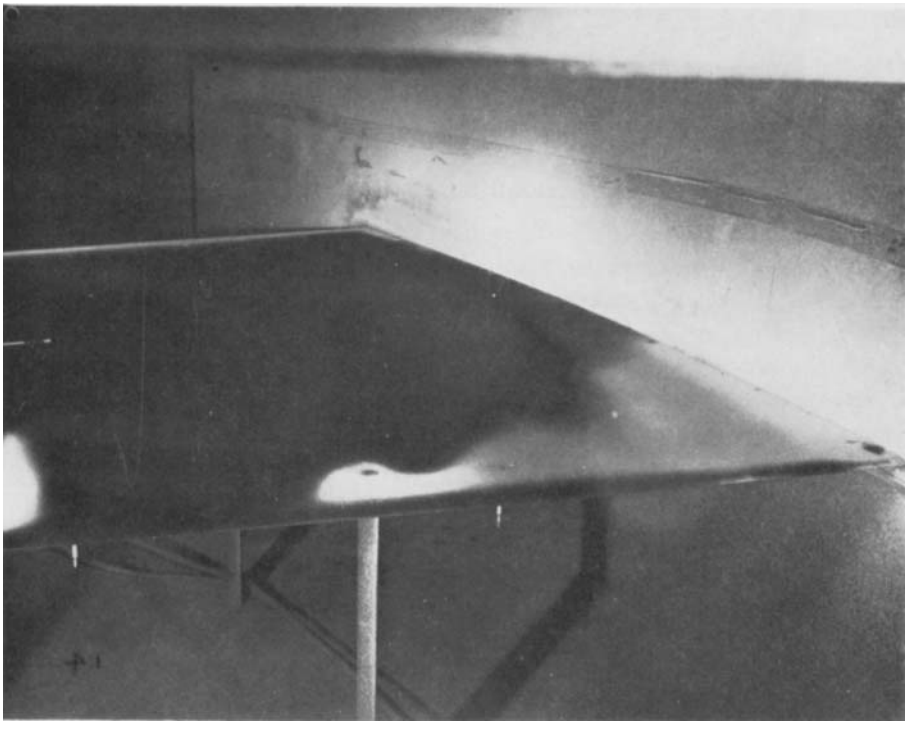

FIGURE 5. Flow visualization with china clay at $U \simeq 30$ ft/s.

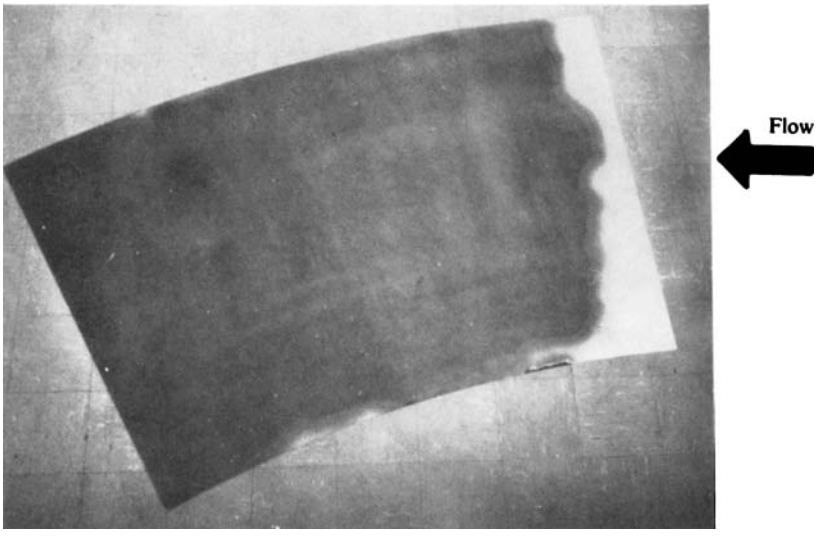

FIGURE 11. Flow visualization with china clay at $U \simeq 10$ ft/s.